Energy Engineering

Tech Science Press

https://doi.org/10.32604/ee.2026.081408

ARTICLE

An Optimisation Method for the Siting and Capacity of Electric Vehicle Charging Stations Considering the User's Charging Accessibility

Bai Xiao[1,*], **Jingjun Bu**[1], **Binbin Du**[2], **Yulin Ge**[2] **and Jian Gao**[2]

[1]Key Laboratory of Modern Power System Simulation and Control & Renewable Energy Technology, Northeast Electric Power University, Ministry of Education, Jilin, China
[2]State Grid Jilin Electric Power Co., Ltd., Changchun Power Supply Company, Changchun, China

*Corresponding Author: Bai Xiao. Email: xbxiaobai@126.com

Received: 01 March 2026; Accepted: 18 March 2026; Published: 30 August 2026

ABSTRACT: In order to solve the problem of the mismatch between the supply of electric vehicle charging stations and charging demand of electric vehicle charging stations caused by the rapid growth of electric vehicles, and the difficulty in determining the optimal site and capacity of electric vehicle charging stations, an optimisation method for the siting and sizing of electric vehicle charging stations considering the accessibility of user charging was proposed. Firstly, the road network topology structure is established in the GIS environment, and the shortest time path of the user is planned by establishing the road impedance model and combining with the improved Dijkstra algorithm. Secondly, Latin hypercube sampling is used to stratify the factors related to EV charging demand, and the spatiotemporal distribution of this demand at each road network node is obtained through Monte Carlo simulation. Based on these spatiotemporal distribution results, the Gaussian Two-step Floating Catchment Area method is adopted to calculate the charging accessibility of electric vehicle users. Subsequently, a siting and sizing model for electric vehicle charging stations is constructed based on the spatiotemporal forecasting of charging demand, and the site selection and capacity optimisation were carried out with the goal of minimising the annual total cost and maximising the charging accessibility evaluation index, so as to balance the interests of both EV charging station investors and electric vehicle users. Finally, a non-dominated sorting genetic algorithm is used to solve the established model, and the entropy weight method and the Technique for Order Preference by Similarity to an Ideal Solution are used to rank the obtained Pareto solution set, and the optimal site selection and capacity determination scheme is selected. An analysis of the results from the proposed method verify the correctness and effectiveness of the proposed optimisation method.

KEYWORDS: Electric vehicle charging stations; Latin hypercubic sampling; spatiotemporal forecasting of charging demand; charging accessibility; optimisation of site selection and capacity; non-dominated sorting genetic algorithm

1 Introduction

As the global fossil energy crisis continues to worsen and environmental pollution becomes increasingly prominent, many countries have formulated the "dual carbon" strategic goals aimed at achieving carbon peaking and carbon neutrality. As a critical hub connecting the two major carbon-emitting sectors of transportation and electric power, the large-scale development of Electric Vehicles (EVs) delivers a dual emission reduction effect [1]. Electric Vehicle Charging Stations (EVCSs) are regarded as key infrastructure for promoting and popularizing EVs. Furthermore, establishing a high-quality charging infrastructure system can more effectively support the growth of the EV industry, stimulate bulk consumption such as EVs, and help achieve the "dual carbon" goals of carbon emission balance [2]. Therefore, the scientific and rational siting and sizing of EVCSs present an urgent demand and important practical significance.

At present, existing research on the siting and sizing of EVCS mainly focuses on two aspects: EV charging load demand forecasting and the establishment of EVCS siting and sizing models.

In terms of EV charging load demand forecasting, references [3,4] established analytical models based on probability and statistics theory, using charging mode, initial state of charge, charging demand, and initial charging time as inputs, and calculated the charging load curve, i.e., the temporal distribution of EV charging demand. References [5–8] fitted the probability distribution of spatiotemporal characteristics at each stage of the electric vehicle travel process, aiming to construct a more accurate spatiotemporal distribution model of charging load. Reference [9] analyzed users' travel behavior based on resident travel statistics and proposed a charging load forecasting method involving travel chain models with varying degrees of complexity. Reference [10] adopted Markov decision theory to dynamically and stochastically simulate travel route choice behavior, thereby predicting the spatiotemporal distribution of charging demand in different regions.

Although the above studies predicted the charging demand in the target area based on the travel chain theory, they did not fully consider the specific structure of the traffic road network and the impact of congestion levels of different road grades on users' route choice. As a result, the forecasting results can hardly accurately reveal the distribution of charging demand at nodes of the road network, which restricts the effectiveness of the optimal layout strategy for electric vehicle charging stations.

In terms of the siting and sizing of EVCS, references [11,12] evaluated the core indicators affecting charging station planning using quantitative analysis methods on the basis of comprehensively considering factors such as land cost and construction cost, and established an EVCS planning model. Reference [13] solved the EVCS siting optimization problem by constructing a total social cost model and a genetic algorithm optimization model. Reference [14] focused on analyzing the relationships between charging station location, capacity, and service scope, and conducted siting and capacity planning to achieve the minimum total annual cost. Reference [15] proposed an approach with the goals of lowering power loss and elevating the voltage profile of the distribution system.

However, in the above siting and sizing models, only indicators affecting the interests of EVCS investors or the power grid were considered, while charging accessibility, a core indicator that can determine the service efficiency of EVCS and characterize the matching degree between the spatial layout of EVCS and the demand distribution of EV users, was not incorporated. As a result, the interests of both EVCS investors and EV users cannot be effectively balanced.

Meanwhile, research on accessibility analysis has mainly focused on fields such as public service facilities and urban science [16–18]. Reference [19] takes the accessibility of medical facilities as a key indicator for measuring the rationality of the spatial layout of medical facilities, providing an important basis for solving problems such as unreasonable allocation and unfair distribution of medical resources. Reference [20] comprehensively considers charging accessibility, total power in the planning area, and electric vehicle charging power. By introducing charging accessibility, the service scope of EVCS can be divided more reasonably and the "range anxiety" of EV users can be alleviated. This method incorporates the charging accessibility of EV users into the siting and sizing model as a constraint, and improves the utilization rate of EVCS to a certain extent. Although high charging accessibility at all nodes is guaranteed, it still fails to accurately distinguish the differences in charging demand at each node and cannot realize the precise matching between charging resources and charging demand, resulting in unreasonable allocation of charging resources.

To address the above problems, this paper proposes an optimization method for the siting and sizing of EVCS considering the charging accessibility of EV users. Firstly, a road impedance model is established by comprehensively considering factors such as road grade, traffic flow, and intersections. Secondly, this paper constructs a novel spatially weighted charging accessibility evaluation index for the first time, which takes the charging demand power of each node as the weight, so as to realize the precise matching between charging facilities and uneven demand distribution. Taking the minimum total annual cost and the maximum charging accessibility evaluation index as optimization objectives, a siting and sizing model of EVCS considering user charging accessibility is developed. Then, the NSGA-II algorithm based on the Pareto dominance relation is adopted to solve the model. Finally, combined with a practical case of a city in Northeast China, the proposed EVCS siting and sizing optimization strategy is proven to be correct and effective based on the obtained results.

2 Algorithm Flow of the Proposed Method

The algorithm flowchart of the optimization method for siting and sizing of EVCS considering charging accessibility of EV users is shown in Fig. 1.

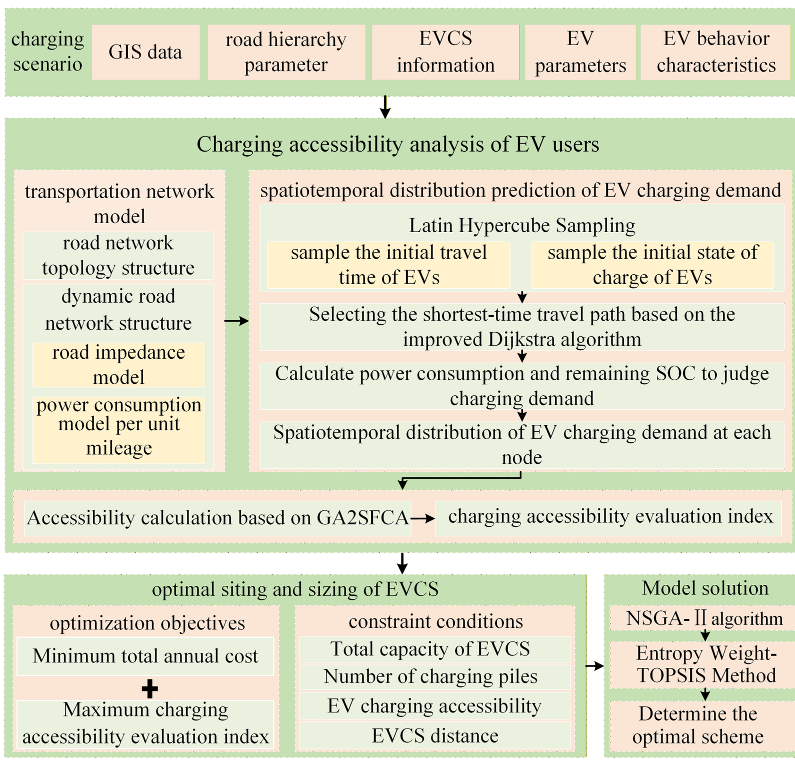

Figure 1: Algorithm flow chart.

1. Analysis of charging scenarios

The charging scenarios in this study are developed from the perspective of multi-stakeholder coordination involved in the planning and construction of EVCSs, including power grid enterprises, municipal departments, and traffic management authorities. Based on GIS traffic data of the target area, and with known parameters of road grade, EVCS information, EV parameters, and travel behavior characteristics of EV users, this paper plans the optimal number, optimal locations, and capacity of EVCS, as well as the allocation of different types of charging piles within stations.

2. Analysis of charging accessibility for EV users

An EV charging demand forecasting model is established. First, a traffic road network model is constructed by analyzing the charging scenario. Second, Latin hypercube sampling is adopted to sample the relevant factors affecting EV charging demand forecasting. The improved Dijkstra algorithm is used to plan the travel path of EVs based on the principle of minimum travel time. Then, the Monte Carlo method is employed to simulate the travel process of EVs, and the remaining state of charge is calculated to determine whether an EV needs charging. Finally, the spatiotemporal distribution of EV charging demand at each road network node is predicted.

A charging accessibility evaluation index for EV users is constructed. The charging accessibility of EV users reflects the convenience of obtaining charging services within a reasonable travel range. According to the results of EV charging demand forecasting, the accessibility of each demand point is calculated using the Gaussian two-step floating catchment area method (GA2SFCA) within a given search radius. Combined with the charging demand and accessibility results at each road network node, the charging accessibility evaluation index for EV users is constructed for the first time via spatial weighting calculation.

3. Establishment of the EVCS siting and sizing optimization model

This paper establishes a bi-objective siting and sizing optimization model, which takes the minimum total annual cost of EVCS and the maximum charging accessibility evaluation index as the optimization objectives. The constraints include the total capacity of EVCS in the planning area, the number of different charging piles in each EVCS, the distance between EVCS, and the charging accessibility of EV users at each demand point.

4. Model solution

To solve the proposed bi-objective optimization model for charging station siting and sizing, the NSGA-II algorithm is applied, and the acquired non-dominated Pareto solutions serve as the candidate scheme set. The weights of the total annual cost and the charging accessibility evaluation index in the alternative scheme set are determined by the entropy weight method. Ultimately, the alternative solutions are evaluated and ranked by means of the TOPSIS method. so as to determine the optimal planning scheme for the siting and capacity allocation of EVCS.

3 Construct a Transportation Network Model

3.1 Construct the Road Network Topology Structure

Based on graph theory, the topological structure of the urban traffic network is constructed by using ArcGIS software. Road intersections (i.e., road network nodes, referred to as nodes for short) are generally represented by an integer sequence $1, 2, \ldots, Y$, where Y is the number of nodes. A directed edge (i, j) denotes a one-way road segment connecting node i to node j. The relationship between nodes and directed edges is described by the adjacency matrix D. Path length, driving speed, travel time, and other parameters are taken as the weights of roads. Directed graphs and undirected graphs are used to represent the traffic structures of one-way streets and two-way streets, respectively. The elements of D are defined as shown in Eq. (1), and the expression of D is given in Eq. (2).

$$d_{ij} = \begin{cases} l_{ij} & \text{directed edge } (i,j) \text{ connects } i \text{ and } j \\ 0 & i = j \\ \infty & \text{Directed edge } (i,j) \text{ is disconnected} \end{cases} \tag{1}$$

$$\boldsymbol{D} = \begin{bmatrix} 0 & l_{12} & \infty & l_{14} \\ l_{21} & 0 & l_{23} & \infty \\ \infty & l_{32} & 0 & l_{34} \\ l_{41} & l_{42} & l_{43} & 0 \end{bmatrix} \tag{2}$$

where: l_{ij} is the length of the road from node i to node j (referred to as the road for short); ∞ denotes infinity, indicating that there is no direct road connection between the two nodes.

In this paper, traffic data of a certain area in a city in Northeast China is obtained from the website (https://www.openstreetmap.org), and the ArcGIS software is used to conduct visual analysis on the traffic data. When constructing the traffic road network, only roads of secondary grade and above are retained, and its topological structure is shown in Fig. 2.

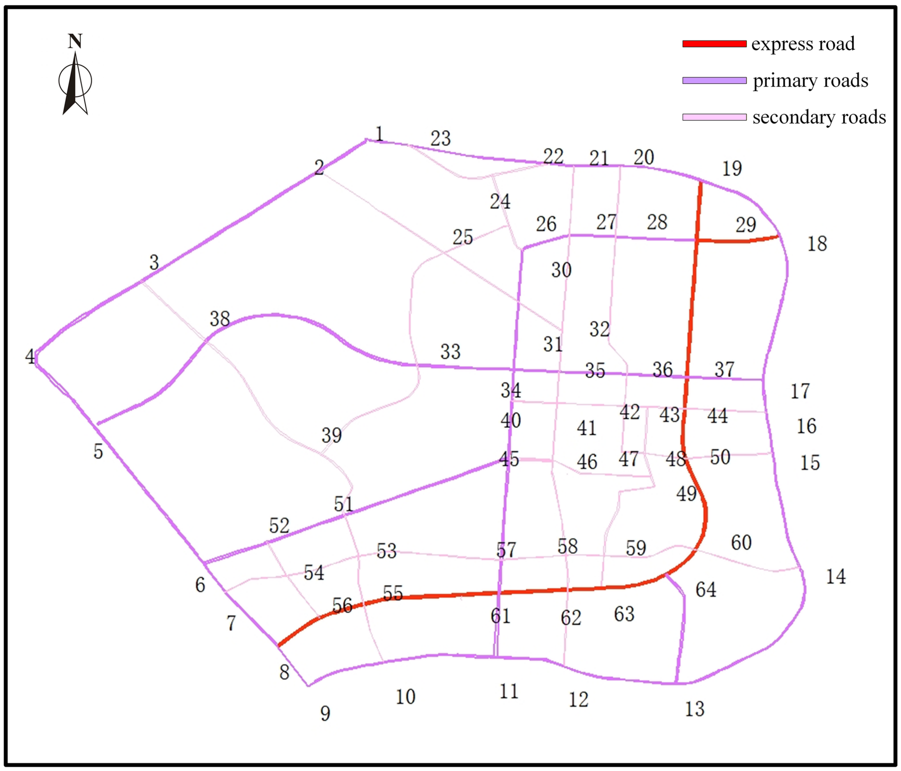

Figure 2: Road network topology.

3.2 *Construct a Dynamic Road Network*

3.2.1 Construct a Road Impedance Model

Considering the impacts of road traffic flow and intersections, EVs inevitably encounter link delays and signalized intersection delays during travel. The road impedance time cost caused by these delays is an important factor that affects users' route choice. Therefore, based on a model from [21], this paper constructs an improved road impedance model to measure this impact. The calculation formula is shown in Eq. (3).

$$T_{ij} = T_{ij.0} + T_{ij.1} \tag{3}$$

where: T_{ij} represents the total time spent by vehicles in road travel; $T_{ij.0}$ is the link impedance, representing the time spent by the vehicle traversing the road segment; $T_{ij.1}$ is the node impedance, representing the travel time of the vehicle at the intersection.

$$\begin{cases} T_{ij.0} = \frac{l_{ij}}{v_{ij}^t} \\ T_{ij.1} = I_0 p_1 \left[1 + \frac{p_2}{1 - e^{\left(p_3 - p_4 \frac{q_{ij}^t}{X}\right)}} \right] \end{cases} \tag{4}$$

where: v_{ij}^t is the speed of the EV on the road at time t; I_0 denotes the free-flow travel time at the intersection; p_1, p_2, p_3 and p_4 are the adaptive coefficients of the signalized intersection; q_{ij}^t represents the traffic flow of different road segments at different times; X denotes the intersection capacity.

To fully consider the differences in road grades, this paper adopts a more accurate speed-flow model that incorporates real-time traffic flow data. This model can describe the driving speed of EVs on roads in detail, so as to predict EV charging demand more accurately. The calculation formula is shown in Eq. (5).

$$\begin{cases} v_{ij}^t = \frac{\tau_1 v_f}{1 + y^{\zeta}} \\ \zeta = \tau_2 + \tau_3 y^3 \end{cases} \tag{5}$$

where: v_f is the design speed for different road grades; τ_1, τ_2, τ_3 and ζ are correction coefficients.

The specific values of each parameter are listed in Table A1 in Appendix A.

The calculation formula for road saturation y is shown in Eq. (6).

$$y = \frac{q_{ij}^t}{c_{ij}} \tag{6}$$

where: c_{ij} denotes the capacity of the designed road segment, which varies with different road grades. The specific values of the parameters are listed in Table A1 in Appendix A.

3.2.2 Construct a Power Consumption Model per Unit Distance

This paper simplifies the calculation process of the energy use per unit travel distance under different road grades [22], and the calculation formula is shown in Eq. (7).

$$W_{ij}^t = \sum_{\alpha=-1}^{2} \beta_\alpha \left(v_{ij}^t\right)^\alpha \tag{7}$$

where: W_{ij}^t is the power consumption per unit mileage on the road *ij* at time *t*; the values of the coefficients β_α are listed in Table A2 in Appendix A.

4 Analysis of Charging Accessibility for EVCS

Charging accessibility refers to the magnitude of spatial resistance overcome by EV users when traveling from any point in space to an EVCS. It reflects the convenience of accessing EVCS charging service resources for EV users within an acceptable range.

4.1 Charging Demand Prediction Based on Latin Hypercube Sampling

EVs are mainly divided into two categories: individual independent decision-making and fleet collective decision-making. Fleet collective decision-making primarily includes commercial operating vehicles including buses and logistics trucks, whose initial departure schedules are relatively fixed, and their trips are mainly determined by the vehicle dispatching center. Individual independent decision-making includes private cars, taxis and other vehicles, where travel and charging behaviors are decided by EV users themselves, with strong individual differences and flexibility. Therefore, this paper only focuses on charging demand prediction for such EVs.

4.1.1 Affecting EV Charging Demand Prediction

(1) Initial departure time

This paper uses the probability distribution curves of initial departure times for different types of EVs on typical workdays provided by the National Cooperative Highway Research Program (https://www.caliper.com/transcad/default.htm). After fitting, the fitted probability density function for private cars is $f_1(t_s)$ and that for taxis is $f_2(t_s)$, with their calculation formulas shown in Eqs. (8) and (9), respectively.

$$f_1(t_s) = 0.8045 + \frac{30.0298}{2.0025\sqrt{\pi/2}} e^{\left[-2\cdot\left(\frac{t_s-7.4103}{2.0025}\right)^2\right]} + \frac{48.4721}{15.2414\sqrt{\pi/2}} e^{\left[-2\cdot\left(\frac{t_s-11.9723}{15.2414}\right)^2\right]} \tag{8}$$

$$f_2(t_s) = 0.1951 + \frac{29.4971}{1.9698\sqrt{\pi/2}} e^{\left[-2\cdot\left(\frac{t_s-6.1780}{1.9698}\right)^2\right]} + \frac{11.9313}{1.7476\sqrt{\pi/2}} e^{\left[-2\cdot\left(\frac{t_s-12.4736}{1.7476}\right)^2\right]} \tag{9}$$

(2) Initial state of charge (SOC)

At the time of initial departure, the SOC values associated with individual EVs are independent of each other. On the basis of the Central Limit Theorem [23], the initial SOC of private vehicles and taxis is assumed to obey the normal distribution N(0.6, 0.1^2), whose probability density function is presented in Eq. (10). During the whole travel process, the real-time SOC is dynamically updated according to the actual driving distance, road grade, and the established power consumption model per unit distance under different traffic conditions. To ensure battery safety and service life, the reasonable operating interval of SOC is constrained within 0.2–0.95. The vehicle will be identified as requiring a charging behavior when the SOC drops to the range of 0.15–0.3 or cannot support the remaining travel demand.

$$f\left(O_S \mid \mu_{soc}, \sigma_{soc}{}^2\right) = \frac{1}{\sigma_{soc}\sqrt{2\pi}} e^{\frac{(O_S-\mu_{soc})^2}{2\sigma_{soc}^2}} \tag{10}$$

where: O_S is the initial state of charge of the EV; σ_{soc} and μ_{soc} are the standard deviation and mean value of the normal distribution followed by the initial SOC of the EV, respectively.

(3) Charging duration

The charging duration of different types of EVs varies significantly with battery capacity and charging power. In this paper, two charging modes (fast charging and slow charging) are selected according to the charging methods and charging sequence preferences of different types of EV users. The calculation formula for EV charging duration is shown in Eq. (11).

$$T_C = \frac{Q\left(0.95 - O_R\right)}{P_C} \tag{11}$$

where: T_C is the EV charging duration; Q is the battery capacity of the EV; O_R is the remaining SOC of the EV; P_C is the charging power selected by the EV.

(4) Parking duration

Due to the special operational nature of taxis, they usually only make short stops at each node for passenger pick-up and drop-off. In contrast, the parking duration of private cars after arriving at their destinations is closely related to the nature of the functional area where they are located. For the parking duration of private cars in work areas, commercial areas and residential areas, this paper adopts the stable distribution, generalized extreme value distribution and Burr XII distribution for modeling, respectively. The specific parameters of each model can be found in Reference [24].

4.1.2 Sampling of Relevant Factors Affecting EV Charging Demand Prediction

To accurately obtain the values of factors affecting EV charging demand and ensure the reliability of subsequent charging demand forecasting, Latin Hypercube Sampling (LHS) is adopted in this paper to conduct stratified sampling for multi-dimensional random variables such as initial departure time and initial SOC, so as to provide reliable input parameters for subsequent travel route planning and Monte Carlo simulation(MCS). Compared with the random sampling method in traditional MCS, when sampling the relevant factors affecting EV charging demand prediction using LHS and MCS, respectively, the former requires fewer sampling times to achieve the same effect as multiple random samplings [25]. As a stratified sampling method, LHS yields highly uniform sampling results and ensures the comprehensiveness of sampling for the factors affecting EV charging demand prediction. Therefore, this paper adopts it to generate parameters such as the initial departure time and initial SOC of EVs.

Considering the actual situation of EV initial trips, the sampling range of initial departure time is set to 0–24 h, and the sampling range of initial SOC is set to 0.2–0.95. The flow chart of sampling relevant factors affecting EV charging demand prediction using LHS is shown in Fig. 3.

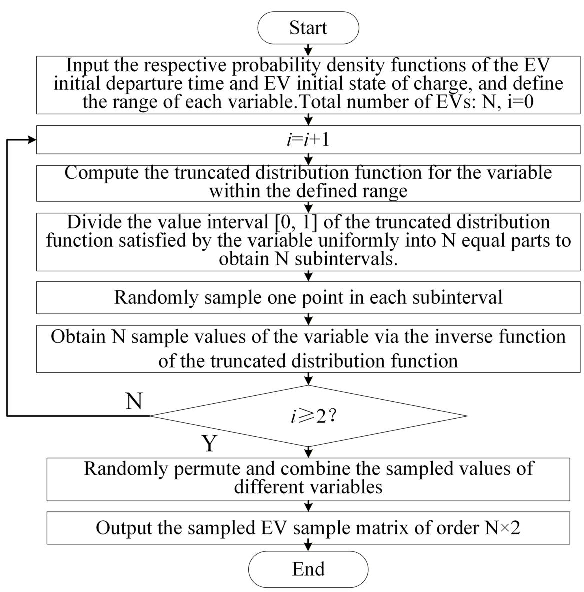

Figure 3: LHS sampling flowchart of factors influencing EV charging demand forecasts.

Using the parameters of influencing factors obtained via LHS, combined with the shortest-time path planned by the improved Dijkstra algorithm, the driving process of EVs can be accurately simulated, thereby realizing the precise prediction of the spatiotemporal distribution of charging demand.

4.1.3 Travel Route Planning

Considering the user's shortest travel route, conventional methods include the Floyd algorithm, Dijkstra algorithm, etc. However, these methods only take the shortest travel distance as the route selection criterion, without considering the impact of additional road impedance time cost on users' route choice caused by link delays and signalized intersection delays during actual EV operation. Therefore, combined with the road impedance model proposed in Section 3.2, this paper uses travel time instead of road length as the element value of the adjacency matrix. The improved Dijkstra algorithm aims to find the route with the shortest travel time from the origin node to the destination node, as shown in Eq. (12), and this route is adopted as the user's travel route.

$$L' = \min L\left(T_{ij}\right), (i, j) \in D \tag{12}$$

where: L' is the shortest-time path from node i to node j.

4.1.4 Prediction Process of Spatiotemporal Distribution of Charging Demand

Based on the influencing factors mentioned in Section 4.1.1, a charging demand prediction model for different types of EVs is constructed. To ensure that EV users have sufficient electricity for the next travel chain and to consider battery lifespan, a safety threshold for SOC is set to maintain the EV SOC within 0.2–0.95.

Thus, this paper assumes that the upper limit of EV SOC during charging does not exceed 0.95. Charging is required when the EV SOC is between 0.15 and 0.3, or when the remaining SOC cannot support the current travel chain. Finally, the spatiotemporal distribution of EV charging demand is predicted via Monte Carlo simulation. The flow chart for predicting the spatiotemporal distribution of EV charging demand is shown in Fig. 4.

Compared with traditional charging demand prediction methods, on the one hand, this paper embeds EV trips into a real road network and calculates power consumption based on real-time link speed, thereby dynamically generating EV charging demand closely correlated with traffic conditions. On the other hand, this paper adopts shortest-time path planning and binds charging demand to the complete travel chain of each vehicle, ensuring that demand prediction is derived from real movement processes.

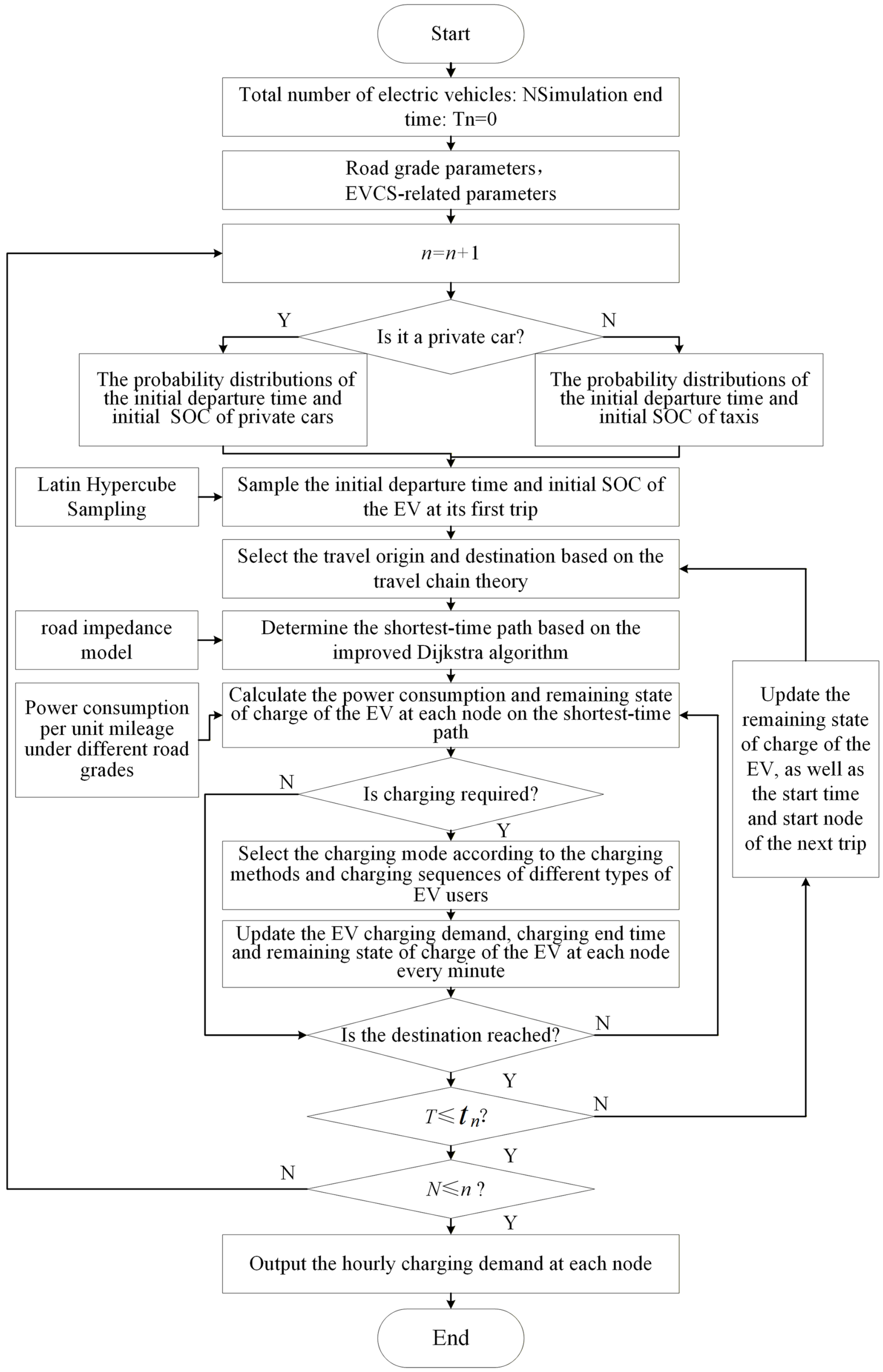

Figure 4: Flow chart of spatio-temporal distribution prediction for EV charging demand.

4.2 Calculation of EV User Charging Accessibility Based on Gaussian Two-Step Search Method

This paper intends to use the Gaussian Two-Step Search Method (GA2SFCA) to calculate the 24-h charging accessibility of EV users assigned to each road network node. The steps are as follows.

(1) The set distance threshold is used as the search radius to statistically analyze the charging demand of road network nodes covered by each candidate charging station. At this time, the formula for calculating the charging demand-supply ratio of each candidate charging station is shown in Eq. (13).

$$R_x = \frac{P_x}{\sum\limits_{y \in \left\{ d_{xy} \le d_o \right\}} G\left(d_{xy}, d_0\right) P_y} \tag{13}$$

$$G\left(d_{xy}, d_0\right) = \begin{cases} \frac{\mathrm{e}-\frac{1}{2}\left(\frac{d_{xy}}{d_0}\right)^2 - \mathrm{e}-\frac{1}{2}}{1-\mathrm{e}\frac{1}{2}}, & d_{xy} \le d_0 \\ 0, & d_{xy} > d_0 \end{cases} \tag{14}$$

where: R_x denotes the charging demand-supply ratio of the x-th EVCS; P_x denotes the rated power of the x-th EVCS; d_{xy} denotes the distance from charging station x to road network node y with charging demand; d_0 denotes the determined distance threshold of charging stations; P_y denotes the predicted value of charging demand at the y-th road network node.

(2) For each road network node, calculate the sum of the charging demand-supply ratios of all candidate charging stations within its search radius coverage, which serves as the charging accessibility of this road network node. The calculation formula is shown in Eq. (15).

$$A_y = \sum_{x \in \left\{ d_{xy} \le d_o \right\}} G\left(d_{xy}, d_0\right) R_x \tag{15}$$

where: A_y is the charging accessibility at road network node y.

The method for calculating charging accessibility in this paper focuses more on spatial service coverage and supply-demand balance, and is especially suitable for scenarios with uneven charging demand distribution and limited resources.

4.3 Construction of Charging Accessibility Evaluation Index

To more comprehensively evaluate the charging accessibility of EV users, this paper constructs for the first time a global evaluation index that measures the charging service level within the entire planning area. The index is weighted based on the charging demand power at each demand node, comprehensively reflecting the charging accessibility of EV users in different regions. Nodes with higher demand have a greater impact of their charging accessibility on the index E. Therefore, to obtain a higher E, more EVCSs will be built near high-demand nodes, and conversely, fewer EVCSs will be deployed near low-demand nodes. This can accurately distinguish the differences in charging demand at each node and realize the precise matching of charging resources with charging demand. The calculation formula is shown in Eq. (16).

$$E = \frac{\sum\limits_{y=1}^{Y} P_y A_y}{\sum\limits_{y=1}^{Y} P_y} \tag{16}$$

where: E is the EV user charging accessibility evaluation index, representing the macro-average charging accessibility of the entire study area, with a value ranging from 0 to 1. The closer to 1, the higher the overall charging service level of the area.

4.4 M/M/c Queuing Theory

Assume that the process of EVs arriving at each EVCS follows a Poisson distribution [26]. Taking the number of EV charging demands arriving at each EVCS per hour as the parameter, the formula for calculating the queuing waiting time of EV users is shown in Eqs. (17)–(19):

$$T_{\mathrm{q}} = \frac{\left(n_{\mathrm{type},x}\delta_{\mathrm{type}}\right)^{n_{\mathrm{type},x}}\delta_{\mathrm{type}}}{n_{\mathrm{type},x}!\left(1-\delta_{\mathrm{type}}\right)^{2}\lambda}P_{0} \tag{17}$$

$$P_{0} = \left[\sum_{n=0}^{n_{\mathrm{type},x}-1}\frac{\left(\lambda/\eta_{\mathrm{type}}\right)^{n}}{n!} + \frac{\left(\lambda/\eta_{\mathrm{type}}\right)^{n_{\mathrm{type},x}}}{n_{\mathrm{type},x}!\left(1-\delta_{\mathrm{type}}\right)}\right]^{-1} \tag{18}$$

$$\delta_{\mathrm{type}} = \frac{\lambda}{n_{\mathrm{type},x}\eta_{\mathrm{type}}} \tag{19}$$

where: T_{q} is the queuing waiting time of EV users; η_{type} is the number of electric vehicles that can be fully charged per unit time by different types of charging piles; δ_{type} is the charging service intensity of different types of charging piles.

5 Bi-Objective Optimization Planning Model for EVCS Site Selection and Capacity Determination

5.1 Objective Function

This paper comprehensively considers the interests of both EVCS investors/operators and EV users. A bi-objective model for site selection and capacity determination is established with the optimization objectives of minimizing the annual total cost of EVCS and maximizing the charging accessibility evaluation index for EV users.

The annual total cost of EVCS consists of two parts: annual construction cost and annual operation and maintenance cost, as defined in Eq. (20):

$$\begin{cases}\min M = M_{1} + M_{2}\\ \max E\end{cases} \tag{20}$$

$$M_{1} = \Phi_{1}\sum_{x=1}^{n_{\mathrm{EVCS}}} r_{x}\left(S_{x}M_{\mathrm{land},x} + e_{\mathrm{type}}n_{\mathrm{type},x} + h_{1}n_{\mathrm{type},x}^{2}\right) \tag{21}$$

$$M_{2} = \Phi_{2}M_{1} \tag{22}$$

$$\Phi_{1} = \frac{\lambda_{0}\left(1+\lambda_{0}\right)^{t_{0}}}{\left(1+\lambda_{0}\right)^{t_{0}}-1} \tag{23}$$

$$S_{x} = 350 + 100n_{\mathrm{type},x} \tag{24}$$

where: M is the annual total cost; M_{1} is the annual construction cost of EVCS; M_{2} is the annual operation and maintenance cost of EVCS; Φ_{1} is the conversion coefficient of annual construction cost; n_{EVCS} is the number of alternative charging stations; r_{x} is the decision variable indicating whether the x-th EVCS is constructed; $n_{\mathrm{type},x}$ is the number of different types of charging piles in candidate charging station x; S_{x} is the land area occupied by candidate charging station x; $M_{\mathrm{land},x}$ is the land purchase price of candidate charging station x in different functional zones, where the price in residential areas is $M_{\mathrm{land,h}}$, in commercial areas is $M_{\mathrm{land,o}}$, and in industrial areas is $M_{\text{land,w}}$; e_{type} is the price of different types of charging piles; h_1 is the equivalent investment factor; Φ_2 is the conversion factor of annual operation and maintenance cost of EVCS; λ_0 is the discount rate; t_0 is the planning period; Y is the total number of road network nodes.

The two objectives in this model are inherently mutually restrictive. When the annual total cost M of EVCS decreases, the charging service scope of EVCS usually shrinks, which reduces users' charging accessibility and results in a lower charging accessibility evaluation index E. Conversely, improving the charging accessibility evaluation index E for EV users requires a higher annual total cost M. Therefore, there is no single optimal solution for this bi-objective optimization problem, but a Pareto optimal solution set that forms the trade-off frontier between the annual total cost M and the charging accessibility evaluation index E. The optimal balance between the interests of investors/operators and EV users is achieved by determining the weights of the two objectives.

5.2 Constraints

(1) Total capacity constraint of EVCS in the planning area

Before configuring the capacity of EVCS, the service scope of each EVCS must first be determined. Based on Ref. [27], this paper takes the behavioral characteristic that EV users prefer the charging station with the shortest travel time as the core basis for delineating the service scope of each EVCS. The aggregate capacity of charging stations in the planning zone should be greater than the projected total EV charging demand, as shown in Eq. (25):

$$\sum_{y=1}^{Y} P_y \le \sum_{x=1}^{n_{\text{EVCS}}} P_x \tag{25}$$

where: P_x is the capacity of the x-th EVCS.

(2) Total power constraint of the planning area

The safety of the power system and grid acceptance capacity must be considered in practical EVCS planning. The sum of the total rated charging power of EVCS and the maximum power of other electrical loads in the planning area shall not exceed the maximum allowable access power of the power grid to ensure its safe operation, as shown in Eq. (26):

$$\sum_{x=1}^{n_{\text{EVCS}}} P_{\text{rated},x} + P_{\text{total,max}} \leqslant P_{\max} \tag{26}$$

where: $P_{\text{rated},x}$ is the rated charging power of the x-th EVCS; $P_{\text{total,max}}$ is the maximum power of electrical loads excluding EV charging load; $P_{\max}$ is the maximum allowable access power of the power grid.

(3) Quantity constraint of charging piles in a single EVCS

Considering traffic flow, regional location, service area scale, investment budget and other factors, the number of different types of charging piles constructed in each EVCS within the planning area must be controlled within a certain range, as shown in Eq. (27):

$$n_{\text{type},x} \leqslant n_{type,max} \tag{27}$$

where: $n_{type,max}$ is the limit of the number of different types of charging piles in a single EVCS.

(4) Construction distance constraint between EVCS

Construction distance constraints are imposed on EVCS in the planning area. An excessively short distance between EVCS will reduce their utilization rate, while an excessively long distance will reduce user satisfaction, as shown in Eq. (28):

$$D_{\min}^{\mathrm{EVCS}} < D^{\mathrm{EVCS}} < D_{\max}^{\mathrm{EVCS}} \tag{28}$$

where: D^{EVCS} is the straight-line construction distance between EVCS; $D_{\min}^{\mathrm{EVCS}}$ is the minimum allowable construction distance between EVCS; $D_{\max}^{\mathrm{EVCS}}$ is the maximum allowable construction distance between EVCS.

(5) Charging accessibility constraint for EV users

The layout planning of EVCS shall ensure that its total service scope fully covers all key nodes in the planning area. The calculation and analysis of the charging accessibility evaluation index for EV users show that an optimization strategy merely pursuing the maximization of the index may lead to an over-bias toward high-demand regions and neglect the basic service guarantee for nodes with low charging demand. Therefore, constraints on the charging accessibility of EV users at each demand node are required.

In planning the number of EVCS, to ensure that each demand node can obtain charging resources and services from at least one EVCS within the search radius, this paper uses a greedy algorithm to gradually increase the number of EVCS and continuously adjust their positions, so as to determine the minimum planned number of EVCS. The minimum value of charging accessibility among all demand nodes at this stage is taken as the threshold in the charging accessibility constraint for EV users, as shown in Eq. (29):

$$A_y \geqslant A_{\mathrm{th}} \quad y = 1, 2, \cdots, Y \tag{29}$$

where: A_{th} is the charging accessibility threshold for EV users.

(6) Queuing waiting time constraint

To ensure that the queuing waiting time of EV users is within an acceptable range and avoid poor user experience caused by excessive waiting time, constraints are imposed on the queuing waiting time of each EV user, as shown in Eq. (30):

$$T_{\mathrm{q}} \leqslant T_{\max} \tag{30}$$

where: $T_{\max}$ is the maximum allowable queuing waiting time for EV users.

6 Determination Solution to the EVCS Site-Selection and Capacity-Determination Model

6.1 Solving the Bi-Objective Optimization Planning Model Using the NSGA-II Algorithm

In this paper, the NSGA-II algorithm is adopted to solve the EVCS site-selection and capacity-determination model, so as to obtain the Pareto frontier containing multiple non-dominated solutions. Each non-dominated solution in the frontier corresponds to an alternative planning scheme. The solution steps are as follows.

Step 1: Parameter setting, including population size, maximum number of iterations and gene coding length. In this paper, a hierarchical hybrid gene coding scheme is adopted: at the spatial layer, the coordinates (longitude, latitude) of candidate EVCS obtained by uniform sampling from road network data are stored; at the decision layer, binary coding is used to represent the construction status of the corresponding candidate

EVCS, where 1 represents construction and 0 represents no construction; at the configuration layer, integer matrix coding is adopted to record the number of fast and slow charging piles at each candidate EVCS.

Step 2: Initialize the iteration counter to 1. The offspring population is generated via crossover and mutation operations. Then merge the parent population and the offspring population, and decode the genotype data of each individual in the mixed population into specific quantity indicators of equipment such as charging piles.

Step 3: Input EV parameters, EVCS parameters, road grade parameters, and the predicted EV charging load demand at each road network node, then calculate the fitness evaluation results of the two optimization objectives.

Step 4: Based on the fitness assessment data of the population in the current iteration, non-dominated sorting and crowding distance computation are implemented, and high-quality individuals with larger crowding distances are preferentially selected to enter the next-generation population.

Step 5: Judge the termination condition, i.e., whether the maximum number of iterations or the convergence condition is reached. If not, repeat Steps 2 to 4 and increase the iteration counter by 1; if yes, output the Pareto frontier.

6.2 Determining Indicator Weights Using the Entropy Weight Method

After obtaining multiple alternative schemes by solving the bi-objective EVCS planning model with the NSGA-II algorithm, it is necessary to determine the weights of each indicator to select the optimal planning scheme. Compared with subjective weighting methods, the entropy weight method, as an objective weighting method, can effectively avoid errors in evaluation results caused by human subjective factors, and the calculation process is simple and efficient.

Suppose there are m alternative EVCS schemes, including k indicators for evaluating the planning schemes. The evaluation indicators of each alternative EVCS scheme are expressed as a vector, denoted as $\boldsymbol{X}_a = \left(x_{a1}x_{a2}\cdots x_{ab}\cdots x_{ak}\right)^{\mathrm{T}}, a = 1, 2, \ldots, m, b = 1, 2, \ldots, k$, forming the original evaluation matrix $\boldsymbol{X} = \left(x_{ab}\right)_{m\times k}$. In this paper, M (annual total cost) and E (charging accessibility evaluation index) are adopted as the evaluation indicators. Since E is a larger-the-better indicator and M is a smaller-the-better indicator, the reciprocal method is first applied to E to unify the directions of the two indicators.

When determining the weights of M and E using the entropy weight method, standardization is required due to their different dimensions and orders of magnitude. The calculation formula is shown in Eq. (31):

$$x_{ab}^{*} = \frac{\max\limits_{b}\left\{x_{ab}\right\} - x_{ab}}{\max\limits_{b}\left\{x_{ab}\right\} - \min\limits_{b}\left\{x_{ab}\right\}} \tag{31}$$

where: x_{ab}^{*} is the standardized value of the b-th indicator of the a-th alternative EVCS scheme; $\max_b\{x_{ab}\}$ is the maximum value of the b-th indicator among all alternative EVCS schemes; $\min_b\{x_{ab}\}$ is the minimum value of the b-th indicator among all alternative EVCS schemes.

The difference coefficient is calculated by Eqs. (32)–(34):

$$\rho_{ab} = \frac{x_{ab}^{*}}{\sum\limits_{a=1}^{m} x_{ab}^{*}}, \left(a = 1, 2, \ldots, m; b = 1, 2, \ldots, k\right) \tag{32}$$

$$H_b = -\frac{1}{\ln\left(m\right)}\sum_{a=1}^{m}\rho_{ab}\ln\left(\rho_{ab}\right) \tag{33}$$

$$g_b = 1 - H_b \tag{34}$$

where: ρ_{ab} is the proportion of the standardized b-th indicator of the a-th alternative EVCS scheme in the total value of this indicator; H_b is the information entropy of the b-th indicator; g_b is the difference coefficient of the b-th indicator.

Finally, the weights of M and E are calculated by Eq. (35):

$$w_b = \frac{g_b}{\sum_{b=1}^{K} g_b} \tag{35}$$

where: w_b is the weight of the b-th indicator.

6.3 Selecting the Optimal Scheme Using the Weighted TOPSIS Method

TOPSIS is a classic multi-criteria decision-making method. Its core idea is that the optimal alternative should be the closest to the positive ideal solution and the farthest from the negative ideal solution. The positive ideal solution consists of the optimal values of each indicator, while the negative ideal solution consists of the worst values. By calculating the relative closeness between each alternative and the ideal solutions, quantitative ranking and optimization selection of the candidate schemes can be achieved. After determining the weights of M and E via the entropy weight method, the TOPSIS method is used to normalize the evaluation matrix to obtain the normalized matrix, and the positive ideal solution (optimal) and negative ideal solution (worst) of M and E among the alternative EVCS schemes are determined.

Finally, the weighted Euclidean distances from each alternative EVCS scheme to the positive and negative ideal solutions are calculated, as well as the relative closeness of each scheme to the positive ideal solution. The alternative EVCS schemes are ranked according to the value of relative closeness, and the optimal EVCS planning scheme is obtained. The specific calculation formulas are shown in Eqs. (36)–(41):

$$z_{ab} = w_b \cdot x_{ab}^{*} \tag{36}$$

$$Z^{+} = \left(z_1^{+}, \cdots, z_b^{+}, \cdots, z_k^{+}\right) \tag{37}$$

$$Z^{-} = \left(z_1^{-}, \cdots, z_b^{-}, \cdots, z_k^{-}\right) \tag{38}$$

$$D_a^{+} = \sqrt{\sum_{b=1}^{n} \left(z_{ab} - z_b^{+}\right)^2} \tag{39}$$

$$D_a^{-} = \sqrt{\sum_{b=1}^{n} \left(z_{ab} - z_b^{-}\right)^2} \tag{40}$$

$$B_a = \frac{D_a^{-}}{D_a^{+} + D_a^{-}} \tag{41}$$

where: $z_b^{+} = \min\limits_{1 \le a \le m} \{z_{ab}\}$; $z_b^{-} = \max\limits_{1 \le a \le m} \{z_{ab}\}$; B_a is the relative closeness of the a-th alternative EVCS scheme to the positive ideal solution, $0 \le B_a \le 1$. The larger the B_a, the better the evaluation of the EVCS planning scheme.

7 Case Study

7.1 Parameter Settings

A case study is conducted based on the actual road network structure of a district in a city in Northeast China. As shown in the road network topology (Fig. 2), the district contains 64 road network nodes and 105 roads. According to points of interest data, the road network nodes are classified into three functional zones: commercial nodes, residential nodes, and industrial nodes, with the detailed classification results presented in Table A3 of Appendix A. The number of electric vehicles in this district is assumed to be 10,000, and their charging demand is predicted accordingly. Among them, private vehicles are Tesla models with a battery capacity of 75 kW·h, totaling 6000 vehicles, while taxis are BYD E5 models with a battery capacity of 60 kW·h, totaling 4000 vehicles. Values of other parameters are provided in Table A4 of Appendix B.

7.2 Analysis of Charging Demand Prediction Results

According to the prediction results, the charging demand in each zone, as illustrated in Fig. 5, exhibits an obvious triple-peak distribution that is highly consistent with urban traffic travel patterns. Starting from 2:00, the EV charging demand in each zone gradually increases. During the morning peak from 5:30 to 7:30, Node 15 in the working area presents a relatively high charging demand with a total of 123 kW·h, corresponding to the concentrated working period and reflecting the typical behavior of commuters charging immediately upon arrival. During the noon peak from 12:00 to 14:00, Node 61 in the commercial zone shows strong charging demand, which reflects the characteristics of commercial activities at noon. During the evening peak from 17:30 to 19:30, Node 35 in the residential zone records a high charging demand of 104 kW·h in total, in line with the daily routine of residents charging after returning home in the evening.

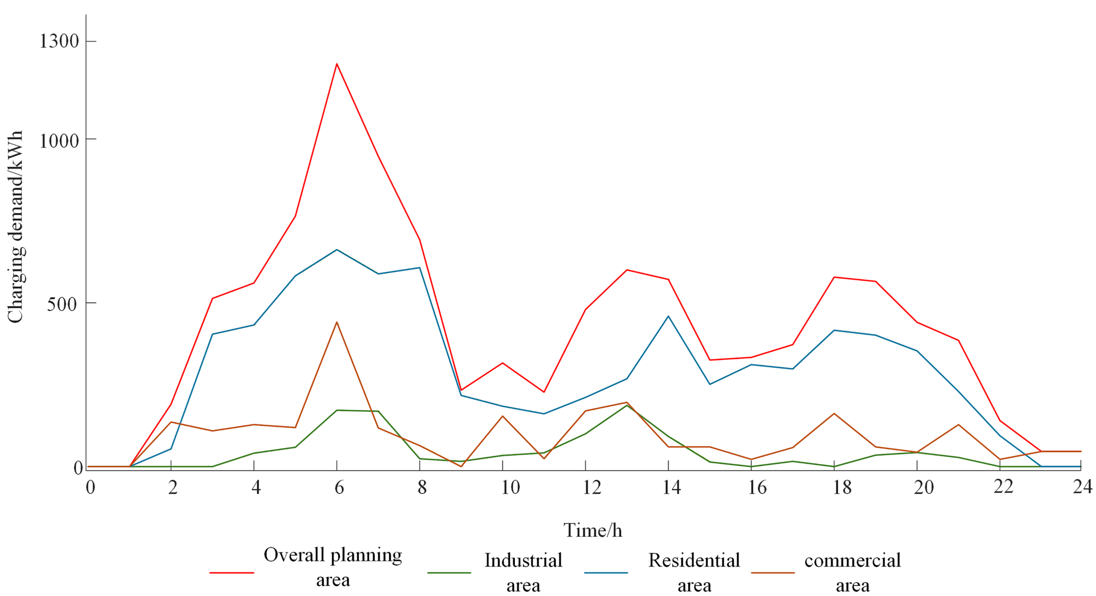

Figure 5: Distribution of charging demand by region.

In addition, based on the road network topology shown in Fig. 2, Node 8 serves as an important hub in the urban traffic network with prominent locational advantages and distinct charging demand characteristics. Located at the intersection of expressways and arterial roads, it acts as a key node connecting the core residential area and surrounding districts of the city. Due to its unique geographical location, Node 8 demonstrates outstanding charging demand performance with an all-day total charging demand of

605 kW·h. The distribution map of charging demand for each road network node is displayed in Fig. A1 of Appendix A.

7.3 Comparison of EVCS Site-Selection and Capacity-Determination Schemes

For the bi-objective optimization planning model for EVCS site selection and capacity determination proposed in this paper, the greedy algorithm indicates that at least 5 EVCSs should be constructed in the planning area. When the number of EVCSs exceeds 8, the annual total cost M will increase significantly with the growing number of EVCSs, while the charging accessibility evaluation index E no longer rises obviously. Excessive deployment of EVCSs tends to result in insufficient facility utilization during periods of low charging demand, thus leading to idle waste of resources.

In the EVCS planning process, the NSGA-II algorithm is applied to obtain solutions for the bi-objective optimization planning model, and the Pareto frontier consisting of 5 EVCS planning schemes for the study area is obtained as alternative schemes. Then, based on the entropy weight method and the values of M and E in the alternative schemes, the weights of M and E are determined as 0.431 and 0.569, respectively. Finally, the TOPSIS method is used to calculate the relative closeness B of each alternative scheme to the optimal ideal solution and rank them accordingly. The comparison results of the alternative EVCS schemes are shown in Table 1.

Table 1: Comparison of EVCS site selection and capacity schemes.

Scheme Number	Number of EVCSs	EVCS Allocation Nodes (Number of Fast Chargers, Slow Chargers/unit)	$M/10^4$ yuan	E	B
1	5	14(12, 1), 51(14, 1), 29(20, 2), 2(8, 1), 50(17, 2)	4047.24	4.839	0.431
2	6	7(10, 1), 29(19, 2), 25(8, 1), 3(10, 1), 14(23, 2), 11(15, 2)	4673.91	5.426	0.441
3	7	29(25, 3), 6(10, 1), 58(10, 1), 32(16, 2), 16(11, 1), 1(12, 1), 13(14, 2)	6412.43	8.856	0.749
4	7	59(22, 2), 16(5, 1), 3(4, 0), 34(23, 3), 39(14, 2), 8(14, 2), 29(21, 2)	7312.51	7.266	0.503
5	8	7(7, 1), 39(13, 1), 46(21, 2), 11(18, 2), 37(8, 1), 23(17, 2), 14(27, 3), 25(14, 2)	7682.98	10.410	0.569

As can be seen from the results in Table 1, Scheme 3 with 7 EVCSs is the optimal EVCS planning scheme, which has the highest relative closeness B to the positive ideal solution. Although the annual total cost M of Scheme 1 and Scheme 2 is better than that of Scheme 3, their charging accessibility evaluation index E is significantly lower than that of Scheme 3. In this case, Scheme 1 and Scheme 2 only satisfy the economic efficiency of EVCS construction without optimizing the charging demand of EV users to the greatest extent.

Compared with Scheme 4, which also deploys 7 EVCSs, Scheme 3 shows a much lower M because all its EVCSs are located at industrial and residential nodes, among which two are planned at industrial nodes where land prices are lower than those in commercial and residential areas, thus well satisfying the economic efficiency of EVCS construction. In Scheme 3, the EVCSs constructed at Node 29 and Node 32 are both located at nodes with high charging demand of EV users, and are equipped with a large number of fast chargers, which enables precise coverage of high-demand nodes and rational allocation of charging resources, resulting in a higher E than Scheme 4.

Compared with Scheme 3, Scheme 5 with 8 EVCSs increases M by 19.8% and E by 17.5%, which improves the rational allocation of EV charging resources to a certain extent, but the construction cost of EVCSs rises sharply. Finally, the weighted calculation by the TOPSIS method shows that Scheme 5 has the second-highest relative closeness B to the optimal ideal solution, just after Scheme 3. The schematic diagram of the closeness degree *B* between different alternatives and the positive ideal solution is shown in Fig. A2, Appendix B.

From the above analysis, Scheme 3 is the current optimal planning scheme. At this time, the charging accessibility of EV users at each node can meet the minimum requirement, and EV users at nodes in high-demand areas can obtain more charging resources, realizing the on-demand allocation of charging resources. Meanwhile, the number of chargers configured in each EVCS is reasonable, reducing the probability of idleness. The interests of both EVCS investors and EV users are effectively balanced. The charging accessibility of EV users at each node under different schemes is shown in Table A5, Appendix B.

7.4 Analysis of Results under Different Planning Objectives

To analyze the impacts of the annual total cost M of EVCS and the charging accessibility evaluation index E of EV users on the planning results, a case with 7 EVCSs constructed is taken as an example. Table 2 shows the comparison of seven typical site-selection and capacity-determination planning schemes.

Table 2: Comparison of typical site selection and capacity planning results.

Scheme Number	Number of EVCSs	EVCS Allocation Nodes (Number of Fast Chargers, Slow Chargers/Unit)	M/10^4 yuan	E	B
1	7	25(10, 1), 56(9, 1), 23(16, 2), 29(9, 1), 41(14, 1), 13(17, 2), 3(20, 2)	6192.25	5.821	0.435
2	7	21(12, 1), 1(9, 1), 63(12, 1), 14(22, 2), 44(23, 3), 39(6, 1), 3(15, 2)	6337.78	6.874	0.526
3	7	29(25, 3), 6(10, 1), 58(10, 1), 32(16, 2), 16(11, 1), 1(12, 1), 13(14, 2)	6412.43	8.856	0.873
4	7	59(22, 2), 16(5, 1), 3(4, 0), 34(23, 3), 39(14, 2), 8(14, 2), 29(21, 2)	7312.51	7.266	0.439

(Continued)

Table 2 (continued)

Scheme Number	Number of EVCSs	EVCS Allocation Nodes (Number of Fast Chargers, Slow Chargers/Unit)	$M/10^4$ yuan	E	B
5	7	7(7, 1), 39(13, 1), 46(21, 2), 11(18, 2), 37(8, 1), 23(17, 2), 14(27, 3)	7489.80	6.215	0.250
6	7	37(15, 2), 25(19, 2), 3(14, 2), 14(23, 2), 8(14, 1), 39(17, 2), 11(19, 2)	7795.05	8.178	0.516
7	7	3(16, 2), 13(25, 3), 39(22, 2), 29(15, 2), 25(25, 3), 15(16, 2), 56(21, 2)	8379.10	9.354	0.564

It can be seen from Table 2 that when only minimizing the annual total cost of EVCS is considered, Scheme 1 is the optimal solution, with an annual total cost M of 6192.25×10^4 yuan and a charging accessibility evaluation index E of 5.821. When only maximizing the charging accessibility evaluation index of EV users is considered, Scheme 7 is the optimal solution, with an annual total cost M of 8379.10×10^4 yuan and a charging accessibility evaluation index E of 9.354.

Based on the entropy weight method and the values of M and E in the typical site schemes, the weights of M and E are determined as 0.436 and 0.564, respectively. The ranking obtained by the TOPSIS method shows that Scheme 3 is the optimal EVCS planning scheme with the highest relative closeness B to the ideal solution, and it is also the optimal solution proposed in this paper that comprehensively considers the interests of both EVCS investors/operators and EV users.

Although the annual total cost M in Scheme 3 is not the lowest, the charging accessibility evaluation index E is 52% higher than that of Scheme 1. Moreover, compared with Scheme 7, although E in Scheme 3 is not the largest, the annual total cost M is reduced by 22.5%, making Scheme 3 the most advantageous among all alternatives. This verifies the superiority of the EVCS site-selection and capacity-determination model proposed in this paper, which fully safeguards the interests of both EVCS investors/operators and EV users.

7.5 Algorithm Comparison

To verify the superiority of the NSGA-II algorithm used in this paper, the NSGA-II and MOPSO algorithms were respectively employed to solve the site selection and capacity determination model for the planning of 7 charging stations within the planning area shown in Fig. 2. Both algorithms were run 50 times, with a population size of 50 and a maximum number of iterations of 100. The C-indicators of the non-dominated solution sets obtained by NSGA-II and MOPSO were compared, and the detailed results are presented in Table 3.

Table 3: Experimental comparison of two algorithms for 7 EVCSs planning scenario.

Statistics of C Indicator	Mean	Standard Deviation
C (NSGA-II, MOPSO)	0.1150	0.0409
C (MOPSO, NSGA-II)	0.0812	0.0474

In terms of the mean value of the C-indicator, the mean of C (NSGA-II, MOPSO) is 0.1150, indicating that 11.50% of the solutions in the MOPSO solution set are dominated by the solutions of NSGA-II, while the mean of II is 0.0812, meaning that only 8.12% of the solutions in the NSGA-II solution set are dominated by the solutions of MOPSO. By comparing the mean results of the two, it can be seen that the non-dominated solution set obtained by NSGA-II is significantly superior to that of MOPSO in overall quality, as it can cover more solutions of MOPSO.

Regarding the standard deviation of the C-indicator, the standard deviation of C (NSGA-II, MOPSO) is 0.0409, which is smaller than 0.0474 of C (MOPSO, NSGA-II). This indicates that during the 50 independent runs, the coverage of NSGA-II over the MOPSO solution set fluctuates less, and the algorithm output is more stable and robust.

It can be seen that the NSGA-II algorithm adopted in this paper improves the solution quality of the model and exhibits superior performance in terms of non-dominated solution set coverage and stability.

8 Conclusions

This paper proposes an optimal siting and sizing method for electric vehicle charging stations considering the charging accessibility of EV users. The method features two innovations:

1. In the EV charging demand prediction stage, the proposed method fully considers the impacts of road traffic flow and intersections on EV user travel, and plans travel paths based on the principle of minimum travel time. This can more realistically reflect the interaction between EV travel behavior and traffic conditions, thereby improving the accuracy of EV charging demand prediction.
2. In the construction stage of the EVCS siting and sizing model, the method innovatively proposes a model that takes user charging accessibility into account. The established charging accessibility evaluation index for EV users can effectively quantify the matching degree between the spatial layout of EVCS and the demand distribution of EV users, and better realize the on-demand allocation of charging resources. As a result, a more economical and satisfactory EVCS siting and sizing scheme can be obtained.

Acknowledgement: I sincerely thank my supervisor Xiao Bai for his careful guidance and valuable professional knowledge throughout the research process, as well as my fellow seniors for their assistance in my scientific research. I also thank Changchun Company for its support. Their joint guidance has played an important role in the successful completion of this study.

Funding Statement: This work is supported by National Key R&D Program of China (2017YFB0902205) and Industrial Innovation Foundation of Jilin Province (2019C058-7).

Author Contributions: The authors contributed to this paper as follows: Jingjun Bu was involved in conceptualization, methodology, software, validation, formal analysis, investigation, resources, data curation, and writing—original draft preparation; Binbin Du, Yulin Ge and Jian Gao participated in validation; Bai Xiao was responsible for supervision, project administration, funding acquisition, and writing—review and editing. All authors reviewed and approved the final version of the manuscript.

Availability of Data and Materials: The data that support the findings of this study are available from the corresponding author upon reasonable request.

Ethics Approval: Not applicable.

Conflicts of Interest: The authors declare no conflicts of interest.

Nomenclature

EVCSs	Electric Vehicle Charging Stations
TOPSIS	Technique for Order Preference by Similarity to an Ideal Solution
EVs	Electric Vehicles
GA2SFCA	Gaussian Two-step Floating Catchment Area
GIS	Geographic Information System
LHS	Latin Hypercube Sampling
SOC	State of Charge

Appendix A

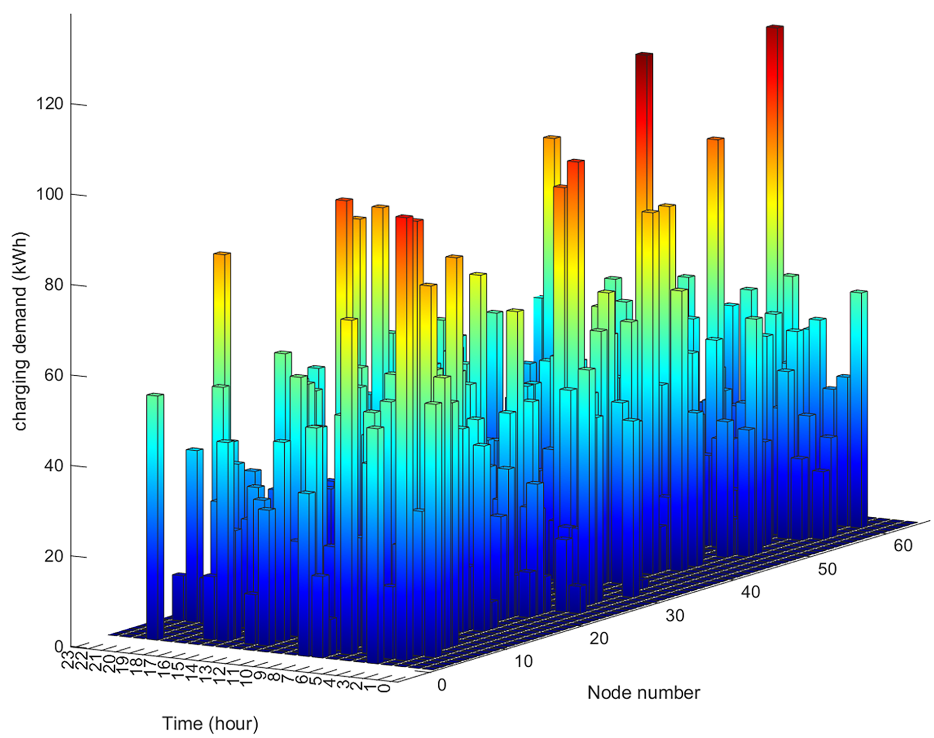

Figure A1: Distribution of charging demand of each network node.

Table A1: Relevant parameters of different road classes.

Road Classification	Design Speed (km/h)	Design Capacity (unit/h)	τ_1	τ_2	τ_3
Express road	80	1750	1.0	1.88	4.90
Primary road	60	1400	1.1	1.89	4.85
Secondary road	40	1300	1.4	1.88	6.97

Table A2: Coefficient of electricity consumption per mile under different road grades.

Road Classification	β_{-1}	β_0	β_1	β_2
Express road	1.520	0.247	−0.004	2.992×10^{-5}
Primary road	5.492	−0.179	0.004	—
Secondary road	1.531	0.210	−0.001	—

Table A3: Functional partitions of road network nodes.

Functional Area	Road Network Node
Residential area	1, 2, 3, 4, 6, 7, 8, 9, 10, 11, 16, 17, 19, 20, 21, 22, 23, 27, 28, 31, 32, 33, 34, 35, 36, 37, 39, 41, 42, 49, 50, 52, 53, 54, 55, 56, 58, 59, 60, 63
Commercial area	5, 12, 18, 24, 26, 30, 38, 40, 43, 45, 47, 48, 57, 61, 62, 64
Industrial area	13, 14, 15, 25, 29, 44, 46, 51

Appendix B

Table A4: Parameter values of case.

Parameter	Value	Parameter	Value
$C_{\mathrm{land}.h}$ (10k yuan/m^2)	5	e_1 (10k yuan)	3
$C_{\mathrm{land}.o}$ (10k yuan/m^2)	8	e_2 (10k yuan)	1
$C_{\mathrm{land}.w}$ (10k yuan/m^2)	3	h_1 (10k yuan)	0.3
P_1 (kW)	120	λ_0	0.08
P_2 (kW)	60	t_0	20
$\boldsymbol{\Phi}_2$	0.1	A_{th}	0.057

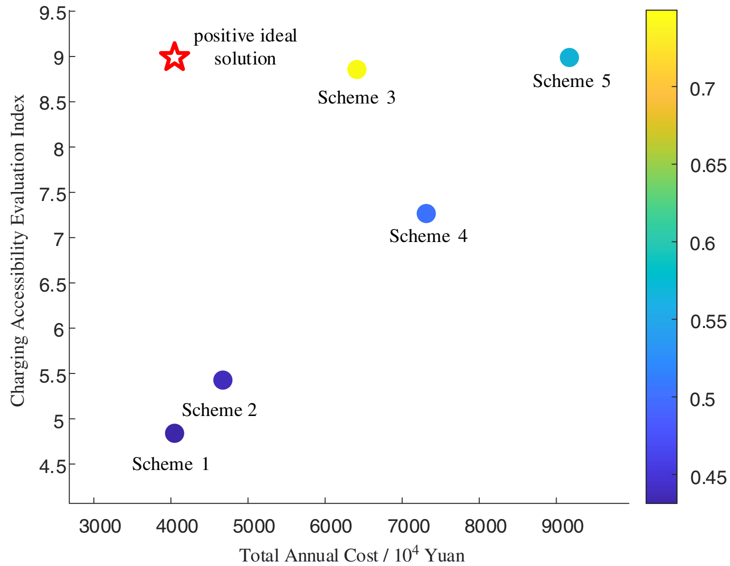

Figure A2: Schematic diagram of the progress of different scheme and the positive ideal solution scheme *B*.

Table A5: Comparison of user charging accessibility at each node under different schemes.

Node	Charging Accessibility for EV Users				
	Scheme 1	Scheme 2	Scheme 3	Scheme 4	Scheme 5
1	0.96	6.65	4.35	0.94	9.42
2	0.51	7.97	4.48	1.57	10.45
3	5.07	5.31	1.39	5.17	2.64
4	6.18	6.12	0.55	1.08	0.47
5	6.57	5.81	1.03	3.89	2.04
6	4.65	3.50	1.44	8.14	4.47
7	3.93	2.51	1.46	7.33	5.34
8	2.28	1.01	1.46	7.45	7.90
9	1.96	0.84	1.18	6.19	8.86
10	4.65	3.25	6.32	8.76	11.25
11	8.94	6.91	15.22	6.45	11.43
12	10.53	8.31	19.84	4.04	14.37
13	11.94	8.68	21.89	2.00	15.92
14	9.39	6.29	18.10	3.31	13.31
15	6.26	3.28	13.24	5.62	13.68
16	4.52	1.70	11.48	6.78	12.19
17	3.30	0.46	9.92	7.52	10.80
18	3.26	1.33	10.38	7.00	2.63
19	3.97	2.67	9.94	6.80	2.73
20	3.64	6.03	9.32	5.74	6.53
21	3.15	7.62	9.24	5.48	8.35
22	2.71	8.37	9.08	5.26	9.22

(Continued)

Table A5 (continued)

Node	Charging Accessibility for EV Users				
	Scheme 1	Scheme 2	Scheme 3	Scheme 4	Scheme 5
23	1.41	6.79	4.77	1.31	9.33
24	2.45	9.86	8.30	4.55	11.66
25	1.90	10.91	4.58	6.75	13.72
26	2.87	10.76	6.18	5.22	13.65
27	3.97	5.31	8.97	5.60	5.66
28	4.42	3.40	9.20	6.27	3.51
29	4.79	1.73	10.94	7.94	1.45
30	3.01	10.33	5.20	3.74	13.04
31	3.18	10.45	5.45	6.66	14.42
32	3.20	9.04	7.65	8.22	12.46
33	2.01	9.57	2.87	10.53	12.56
34	2.96	9.10	6.85	11.14	16.05
35	3.32	7.98	9.14	11.68	13.03
36	3.93	4.82	11.30	10.95	9.34
37	6.75	4.44	16.79	11.09	9.82
38	3.54	5.23	0.26	8.25	3.75
39	2.07	5.96	1.66	12.55	10.38
40	2.73	8.25	5.56	9.85	15.45
41	3.13	7.01	8.33	10.19	12.31
42	4.21	4.46	11.87	9.98	9.78
43	5.70	4.33	14.86	10.64	10.25
44	7.90	4.20	18.75	10.66	10.42
45	2.85	6.43	4.29	10.23	15.14
46	4.94	6.90	9.40	9.37	13.86
47	5.98	4.40	13.67	8.69	10.94
48	7.29	4.58	16.63	9.32	12.48
49	6.96	4.16	15.76	9.09	12.22
50	9.42	5.33	20.73	9.33	12.24
51	2.76	4.11	2.03	13.25	11.89
52	3.35	2.28	1.63	9.84	7.10
53	2.80	2.33	2.11	12.91	11.42
54	2.62	1.39	1.85	9.60	7.77
55	2.50	1.63	1.82	11.26	11.32
56	2.47	1.23	1.69	9.43	8.95
57	6.17	5.39	9.53	10.81	16.42
58	9.04	6.47	15.31	7.58	17.00
59	8.29	5.62	14.28	5.65	16.96
60	11.60	7.44	22.00	5.92	17.03
61	6.99	5.51	11.60	9.51	14.52
62	9.65	7.16	16.87	6.04	16.32

(Continued)

Table A5 (continued)

Node	Charging Accessibility for EV Users				
	Scheme 1	Scheme 2	Scheme 3	Scheme 4	Scheme 5
63	9.93	7.21	17.63	4.69	16.79
64	12.24	8.18	21.75	4.17	17.03

References

1. Li B, Zhao Y, Wei Y. Research on key supporting technologies for demand-side resource interaction in the context of carbon neutrality. Distrib Util. 2021;38(9):3–9. doi:10.19421/j.cnki.1006-6357.2021.09.001.
2. Rivera S, Kouro S, Vazquez S, Goetz SM, Lizana R, Romero-Cadaval E. Electric vehicle charging infrastructure: from grid to battery. EEE Ind Electron Mag. 2021;15(2):37–51. doi:10.1109/mie.2020.3039039.
3. Luo ZW, Hu ZC, Song YH. Calculation method for charging load of electric vehicles. Power Syst Autom. 2011;35(14):36–42.
4. Calearo L, Thingvad A, Suzuki K, Marinelli M. Grid loading due to EV charging profiles based on pseudo-real driving pattern and user behavior. IEEE Trans Transp Electrif. 2019;5(3):683–94. doi:10.1109/TTE.2019.2921854.
5. Zhang Q, Zhu Y, Wang Z, Su Y, Li C. Reliability assessment of distribution network and electric vehicle considering quasi-dynamic traffic flow and vehicle-to-grid. IEEE Access. 2019;7:131201–13. doi:10.1109/ACCESS.2019.2940294.
6. Liang H, Lee Z, Li G. A calculation model of charge and discharge capacity of electric vehicle cluster based on trip chain. IEEE Access. 2020;8:142026–42. doi:10.1109/ACCESS.2020.3014160.
7. Tao S, Liao K, Xiao X, Wen J, Yang Y, Zhang J. Charging demand for electric vehicle based on stochastic analysis of trip chain. IET Gener Trans Dist. 2016;10(11):2689–98. doi:10.1049/iet-gtd.2015.0995.
8. Yang P, Cao Y, Tan J, Chen J, Zhang C, Wang Y, et al. Electric vehicle charging capacity of distribution network considering conventional load composition. Energy Eng. 2023;120(3):743–62. doi:10.32604/ee.2023.024128.
9. Wang W, Tang A, Wei F, Yang H, Li X, Peng J. Electric vehicle charging load forecasting considering weather impact. Appl Energy. 2025;383:125337. doi:10.1016/j.apenergy.2025.125337.
10. Tang D, Wang P. Probabilistic modeling of nodal charging demand based on spatial-temporal dynamics of moving electric vehicles. IEEE Trans Smart Grid. 2016;7(2):627–36. doi:10.1109/TSG.2015.2437415.
11. Ren X, Zhang H, Hu R, Qiu Y. Location of electric vehicle charging stations: a perspective using the grey decision-making model. Energy. 2019;173(6):548–53. doi:10.1016/j.energy.2019.02.015.
12. Guindi M, Kamel RM. Optimal location and sizing of renewable distributed generations and electric vehicle charging stations. Renew Energy. 2024;235:121272. doi:10.1016/j.renene.2024.121272.
13. Zhou G, Zhu Z, Luo S. Location optimization of electric vehicle charging stations: based on cost model and genetic algorithm. Energy. 2022;247:123437.
14. Liu Z, Wen F, Ledwich G. Optimal planning of electric-vehicle charging stations in distribution systems. IEEE Trans Power Deliv. 2013;28(1):102–10. doi:10.1109/TPWRD.2012.2223489.
15. Tian MY, Tang B, Yang X, Xia XW. Planning of electric vehicle charging stations considering charging demands and acceptance capacity of distribution network. Power Syst Technol. 2021;45(2):498–506. (In Chinese).
16. Tahmasbi B, Mansourianfar MH, Haghshenas H, Kim I. Multimodal accessibility-based equity assessment of urban public facilities distribution. Sustain Cities Soc. 2019;49:101633. doi:10.1016/j.scs.2019.101633.
17. Zhang R, Peng S, Sun F, Deng L, Che Y. Assessing the social equity of urban parks: an improved index integrating multiple quality dimensions and service accessibility. Cities. 2022;129(3):103839. doi:10.1016/j.cities.2022.103839.
18. Verduzco Torres JR, McArthur DP. Public transport accessibility indicators to urban and regional services in Great Britain. Sci Data. 2024;11(1):53. doi:10.1038/s41597-023-02890-w.
19. Xu M, Liao Q, Xie ZM. Spatial accessibility evaluation of rural medical facilities in southwest mountainous area: taking Jiulongpo district, Chongqing municipality as an example. J Hum Settl West China. 2024;39(5):50–6. (In Chinese).

20. Liu DL, Wang YF, Zhang Y, Xue H, Mi Y, Yu AQ. Siting and sizing method of electric vehicle charging stations based on Huff model. Electr Power Autom Equip. 2023;43(11):103–10. (In Chinese). doi:10.1109/ievc.2012.6183283.
21. Lu T, Yang Z, Ma D, Jin S. Bi-level programming model for dynamic reversible lane assignment. IEEE Access. 2018;6:71592–601. doi:10.1109/ACCESS.2018.2881290.
22. Song YN, Lin SJ, Tang ZQ. Spatialtemporal distribution probabilistic modeling of electric vehicle charging load based on dynamic traffic flow. Autom Electr Power Syst. 2020;44(23):47–56. doi:10.7500/AEPS20200302005.
23. Arias MB, Bae S. Electric vehicle charging demand forecasting model based on big data technologies. Appl Energy. 2016;183(2):327–39. doi:10.1016/j.apenergy.2016.08.080.
24. Zhang J, Yan J, Liu Y, Zhang H, Lv G. Daily electric vehicle charging load profiles considering demographics of vehicle users. Appl Energy. 2020;274(2):115063. doi:10.1016/j.apenergy.2020.115063.
25. Abyani M, Bahaari MR. A comparative reliability study of corroded pipelines based on Monte Carlo simulation and latin hypercube sampling methods. Int J Press Vessels Pip. 2020;181(4):104079. doi:10.1016/j.ijpvp.2020.104079.
26. Alharbi T, Abdalrahman A, Mostafa MH. Data-driven EV charging infrastructure with uncertainty based on a spatial-temporal flow-driven (STFD) models considering batteries. Sci Rep. 2025;15(1):27056. doi:10.1038/s41598-025-12079-3.
27. Xiao B, Gao F. Optimization method of electric vehicle charging stations' site selection and capacity determination considering charging piles with different capacities. Electr Power Autom Equip. 2022;42(10):157–66. (In Chinese). doi:10.16081/j.epae.202207001.